**OPEN ACCESS*****Correspondence:**

Uloko, P. I.

Email:patrickin05jesus@gmail.com**Specialty Section:**

This article was submitted to Sciences, a section of NAPAS.

Submitted: 9 April 2022**Accepted:** 18 August, 2022**Published:** 15 Nov. 2022**Citation:**

Akiishi, M., Uloko, P. I. and Ichagba A (2022).

Identification of Depth to Basement and Mineral Deposits in Monguno Area Northeastern Nigeria Using Source Parameter Imaging and Modeling Technique. *Nig Annals of Pure & Appl Sci.* 5(2):413-421. DOI: 10.5281/zenodo.7783347

Publisher:

cPrint, Nig. Ltd

E-mail: cprintpublisher@gmail.com**Access Code**<http://napas.org.ng>

Identification of Depth to Basement and Mineral Deposits in Monguno Area Northeastern Nigeria Using Source Parameter Imaging and Modeling Technique

Akiishi, M., Uloko, P. I* and Ichagba A.

College of Education Oju, Benue State, Nigeria.

ABSTRACT

High resolution aeromagnetic (HRAM) and aerogravity data covering Monguno was interpreted qualitatively and quantitatively. Regional - residual data separation enhancement technique or residual from deeply seated magnetic and gravity bodies were taken to discriminate shallow related sources. The residual magnetic values obtained were used to produce the residual magnetic map, while the residual gravity values were used to produce residual bouguer anomaly map. The qualitative interpretation depicts that the area is characterized by low and high frequency magnetic and gravity signatures. The aeromagnetic source parameter imaging indicates sedimentary thickness value of about 3259.4 m, while aerogravity source parameter imaging reveals sedimentary thickness value of about 4674.3 m. These sedimentary thicknesses obtained are indication that the area could have potential of hydrocarbon accumulation. On the other hand, forward and inverse modeling was carried out using aeromagnetic data. It estimates the basement depth for P1 and P2 as 2296 and 1321m respectively with corresponding magnetic susceptibility values of 0.0170 and 0.0100, which indicate the possibility of economic mineral deposits, such as: Sandstone and Shale in the area. Furthermore, aerogravity forward and inverse modeling technique estimates the depth to basement for P1 as 1729 m, with corresponding density value of 2.510 g/cm³ which depicts the possibility of having mineral deposits, such as: kaolinite and gypsum in the area. The results obtained in this work show that petroleum exploration and ceramic companies could be sited in the area. This will provide employment opportunity in the area; and the socio economic life of the people will be greatly improved.

Keywords: aeromagnetic, aerogravity data, forward and inverse modeling, sedimentary thickness, Oasis Montaj 6.4.2 and potent Q. source parameter imaging.

INTRODUCTION

Nigerian population keeps increasing on a daily basis. As a result, her financial demand continues to raise, hence the need for an alternative source of revenue generation such as the revenues drive from the sale of mineral resources. Nigeria is blessed with a lot of mineral deposit (Obaje, 2009), though majority are untapped. These mineral deposits, if harnessed and commercialized could improve the country's wealth. However, over the years, the country's wealth has been depending on revenue generated from the sale of crude oil (Salako, 2014; Obiora, 2015), which is mostly explored in the southern part of the country. Therefore there is the fear that it may soon be exhausted. In addition, the communal crises in the area as a result of resource control have led to the destruction of public and private properties, thereby affecting the economic development of the country as well as her unity. More so, the kidnapping of oil workers in the region has led to the closure of many oil companies. Hence these could lead to low production of crude oil, which may subsequently result to scarcity of petrol, thus leading to increase in transportation fare, prices of goods and services. This situation could cause hardship to the masses and thus projects negative image of the country. With more crude oil exploration areas and government subsidizing other factors, many oil companies will go into much production of crude oil and this could help in reducing scarcity of fuel in the country. Therefore, this research work investigates mineral deposit and depth to basement in Monguno area, which is one of the towns in the Northeastern Nigeria that posses geological features that encourages accumulation of hydrocarbon and mineral deposit (Adekoya *et al.*, 2014). Research works have been carried out in the study area; however such works combined the aeromagnetic data of Monguno and other areas (Akiishi and Ankeli, 2020, Akiishi *et al* 2019, Kehinde *et al.*, 2019, Adewumi *et al.*, 2019, Sani *et al.* 2018, Ayigun *et al.*, 2022, Mwobodo *et al.* 2021,

Rabo *et al.* 2021, Udochukwu *et al.*, 2019 and Ijeh *et al.*, 2019). This might not have given adequate geological information of the area, since some geological features in the area might be masked by geological features of other areas. Secondly, most of these works were centered on geothermal energy sources and water sources identification. Finally, this work uses aeromagnetic and aerogravity data so that depth to basement comparison could be made in order to ascertain good sedimentary thickness capable of producing crude oil, similarly, any mineral deposit that may not respond to magnetic influence could be identified base on its gravity.

2.0 Location and Geology of the Study Area

Monguno is located in Nigerian sector of Chad basin (lat. 12° 00' to 13° 00' and long 12° 30' to 14° 00'). The Nigerian sector of Chad basin is about one tenth of the Chad basin and has a broad sediment-filled depression spanning north eastern Nigeria and adjoining parts of the Republic of Chad. The area generally is endowed with rock mineral base resources such as clay, salt, limestone, kaolin, iron ore, uranium, mica etc (Ajana *et al.*, 2014), The sedimentary rocks of the area have cumulative thickness of over 3.6 km and the rocks consist of thick basal continental sequence overlaid by transitional beds followed by a thick succession of quaternary Limnic, fluvatile and eolian sand, clay etc (Odebode , 2010). The stratigraphic sequence shows that Chad, Kerri-Kerri and Gombe formations have an average thickness of 130 to 400 m. Below this formations are the Fika shale with a dark grey to black in colour, with an average thickness of 430 m. Others are Gongila and Bima formations with average thicknesses of 320 and 3500 m, respectively (Odebode, 2010, and Okosun, 1995).

3.0 Source of Data

The high resolution airborne magnetic data and gravity data used in this study were obtained from

Nigerian Geological Survey Agency (NGSA). The airborne gravity data were obtained using GRACE GRAVITY MODEL Sensor onboard 2 satellites by National Aeronautics and Space Administration (NASA) and German Aerospace Center in 2013, while the aeromagnetic data were obtained using a 3 x Scintrex CS2cesium vapour magnetometer by Fugro Airborne Surveys in 2009. The airborne magnetic survey was carried out at 80 m elevation along flight lines spaced 500 m apart. The flight line direction was 135°, while the tie line direction was 225°. A correction based on the international Geomagnetic Reference Field (IGRF) 2010 was applied.

3.1 Theory of Source Parameter Imaging

The source parameter imaging (SPI) uses an extension of the complex analytical signal to estimate magnetic source depths, source geometries, the dip and susceptibility contrast. It has the advantage of producing a more complete set of coherent solution points and it is easier to use than other depth mapping techniques such as the Euler deconvolution technique.

The method estimates the depth from the local wave number of the analytical signal. The analytical signal

($A_1(x, z)$) is defined by Nabighian (1972) as:

$$A_1(x, z) = \frac{\partial M(x, z)}{\partial x} - j \frac{\partial M(x, z)}{\partial z} \tag{1}$$

where, $M(x, z)$ is the magnitude of the anomalous field, j is the imaginary number, and z and x are Cartesian coordinates for the vertical and the horizontal directions perpendicular to strike, respectively. Nabighian (1972) showed that the horizontal and vertical derivatives comprising of the real and imaginary parts of the 2D analytical signal are related by the expression,

$$\frac{\partial M(x, z)}{\partial x} \Leftrightarrow -j \frac{\partial M(x, z)}{\partial z} \tag{2}$$

where the \Leftrightarrow denotes a Hilberts transform pair. The Local wave number K_1 is defined by Thurston and Smith (1997) as:

$$k_1 = \frac{\partial}{\partial x} \tan^{-1} \left[\frac{\frac{\partial M}{\partial z}}{\frac{\partial M}{\partial x}} \right] \tag{3}$$

The analytic signal involves second order derivative of total field, if used in a manner similar to that used by Hsu *et al.* (1996). The Hilbert transform and the vertical derivative operator are linear, so the vertical derivative of equation (2) will give the Hilbert transform pair.

Thus, the analytic signal could be defined based on second-order derivatives,

$A_2(x, z)$, where

$$A_2(x, z) = \frac{\partial^2 M(x, z)}{\partial z \partial x} - j \frac{\partial^2 M(x, z)}{\partial^2 z} \tag{4}$$

This gives rise to a second-order local wave number K_2 , where

$$K_2 = \frac{\partial}{\partial x} \tan^{-1} \left[\frac{\frac{\partial^2 M}{\partial^2 z}}{\frac{\partial^2 M}{\partial z \partial x}} \right] \tag{5}$$

Thus, the expressions in equations 3 and 5 imply that the SPI utilizes the relationship between source depth and the local wave number (K) of the observed field, which can be calculated for any point within a grid of data via horizontal and vertical gradients (Thurston and Smith, 1997)

Forward and inverse modeling

Forward and inverse modeling is a trial and error method, the shape, position and physical properties of the model are adjusted in order to obtain a good correlation between the calculated field and the observed field data. Using Potent Q 3D tool of the Oasis Montaj software, the field of the model was calculated.

3.2 Methods of Data interpretation

3.2.1 Qualitative interpretation

The total magnetic intensity and Bouguer anomaly data were separately imported into Oasis Montaj 6.4 software and were subsequently gridded using minimum curvature. These gridded data were further used to produce the total magnetic intensity and Bouguer anomaly maps. The regional - residual separation was carried out by first order polynomial fitting. The residual values of both magnetic and Bouguer anomalies were used to produce the residual magnetic intensity and residual gravity anomaly maps.

3.2.2 Quantitative interpretation

3.2.2.1 Source parameter imaging

The first and second order local wave numbers were used to determine the most appropriate model and depth estimate of any assumption about a model. Oasis Montaj software was employed to compute the SPI image and depth using equations (1) – (5)

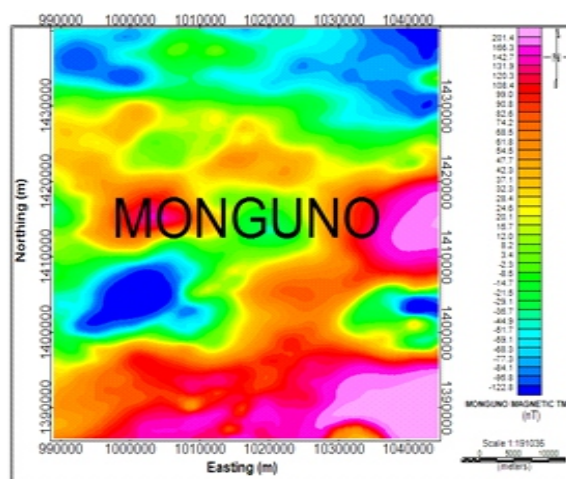
3.2.2.2 Forward and inverse modeling

Two profiles were taken on the residual magnetic map and one profile on the Bouguer anomaly map and modeled. Each profile produced a degree of

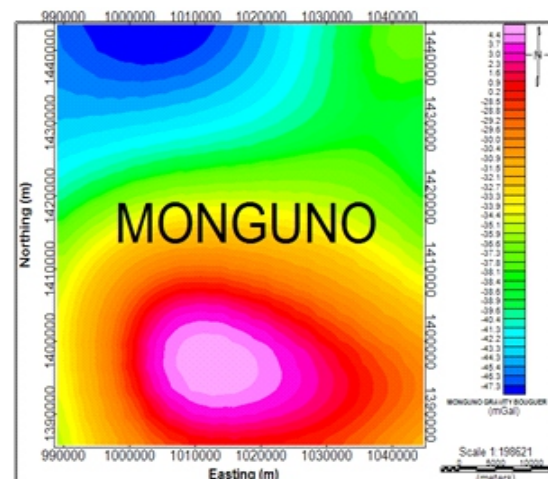
strike, dip and plunge where the observed values matched well with the calculated values. The blue curves represent the observed field values, while the red curves represent the calculated field values. The root mean square (RMS) difference between the observed and calculated field values were minimized by the inversion algorithm. At the end of the inversion, the RMS value was displayed. The RMS value decreased as the fit between the observed and calculated field continues to improve, until a reasonable inversion result was achieved. Less than 5% of root mean square value was set as the error margin.

4.0 RESULTS

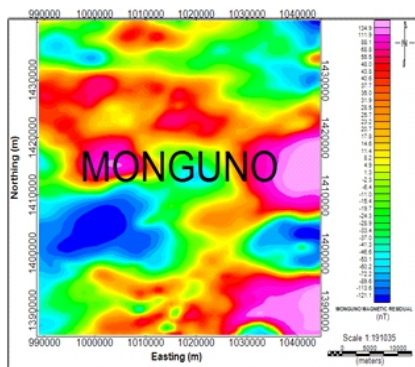
Figure 1 shows the total magnetic intensity and the residual magnetic maps of the area, while Figure 2 presents the division of the residual magnetic map into 9 equal spectral cells for estimation of geothermal parameters. Figures 3 and 4 give the spectral plots of logarithm of energy against frequency for cells 1-4 and 5-9 respectively. The estimated geothermal parameters of the area are recorded on Tables 2. On the other hand, Figure 5 presents the contour maps of geothermal parameters of Monguno area.



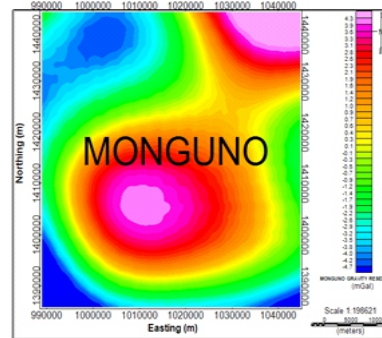
(a) Total magnetic intensity (TMI) map



(b) Bouguer gravity anomaly map

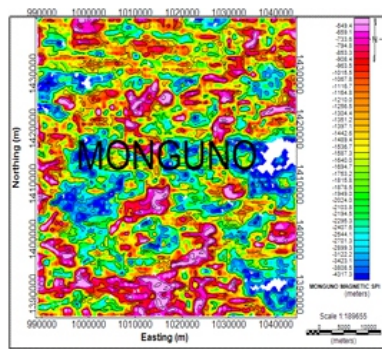


(c) Residual magnetic anomaly map

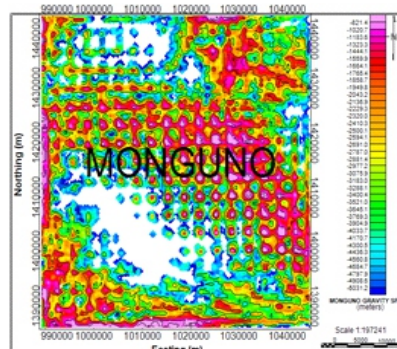


(d) Residual bouguer anomaly map

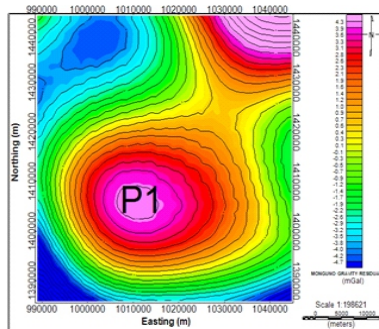
Fig. 1 Maps Showing Results of Qualitative Interpretation of Aeromagnetic and Aerogravity Data for Monguno



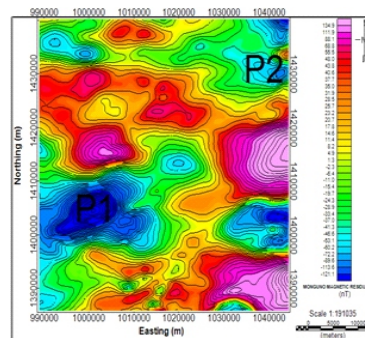
(a) Aeromagnetic source parameter imaging (SPI) depth Map



(b) Aerogravity source parameter Imaging (SPI) depth map



(c) Aeromagnetic residual contour map showing two profile locations



(d) Aerogravity residual contour map Showing one profile location

Fig. 2 Maps showing source parameter imaging and profiles location in Monguno

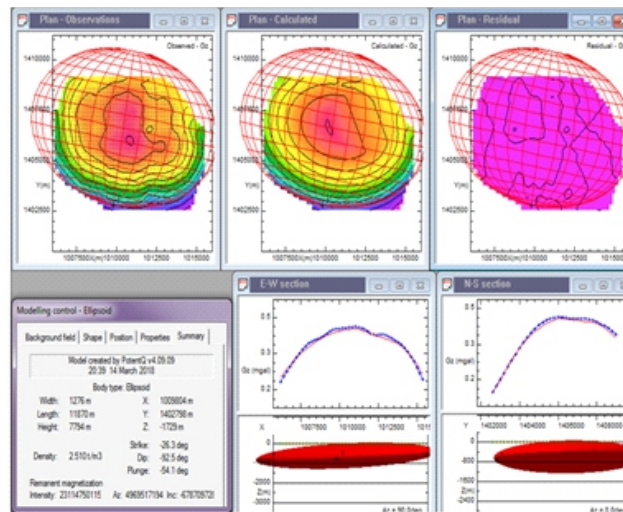
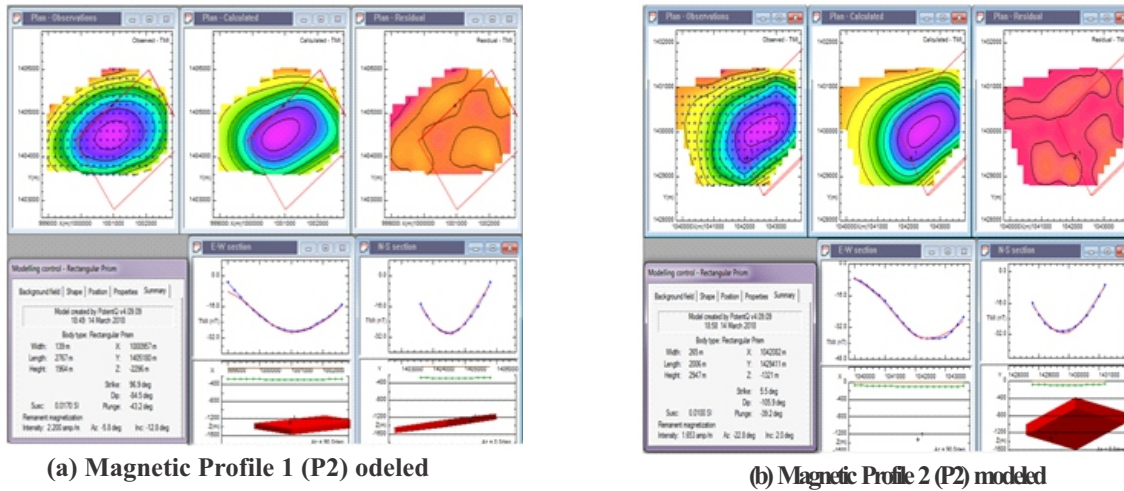


Fig.3: Modeled Profiles for Aeromagnetic and Aerogravity data

Table 1: Summary of Aeromagnetic Forward and Inverse Modeling Results of Monguno

Model	Model shape	X(m)	Y(m)	Depth to anomalous body (m)	Plunge (deg)	Dip (deg)	Strike (deg)	χ (SI)	Possible cause of anomaly
P1	Rectangular Prism	1000957	1405180	2296	-43.2	-84.5	96.9	0.0170	Sandstone
P2	Rectangular Prism	1042082	1429411	1321	-39.2	-105.9	5.5	0.0100	Shale

Table 2: Summary of Aerogravity Forward and Inverse Modeling Results of Monguno

Model	Model shape	X(m)	Y(m)	Depth to anomalous body (m)	Plunge (deg)	Dip (deg)	Strike (deg)	Density value (g/cm ³)	Possible cause of anomaly
P1	Ellipsoid	1009804	1402798	1729	-54.1	-92.5	-26.3	2.510	Kaolinite/ Gypsum

DISCUSSION

Total magnetic intensity map (Fig. 1a) of the study area shows magnetic intensity of the area ranges from -122.8 to 201.4 nT. This indicates the study area is characterized by low and high frequencies magnetic signatures. Magnetic signature of low frequency dominates the northern part of the area; this implies relatively high depth to basement in the northern part of the area, while high magnetic signatures are observed in southern part, indicating relatively shallow depth. The low magnetic signature in the area could be attributed to deep-seated magnetic bodies, while high frequency magnetic signature could be due to intrusion or near surface magnetic bodies. This agrees with Rabo *et al.* (2021) who observed that high magnetic anomaly in most parts of Chad Basin is as a result of intrusions of magnetic bodies.

Observations from Figure 1b show Bouguer anomaly of the area varies from -47.3 to 4.4 mGal. High Bouguer anomaly observed in southern part of the area implies the intruded crystalline basement rocks in the region is highly dense. Meanwhile low Bouguer anomaly noticed in the northern area, signifying low in dense sediment in the area is. The high and low Bougure anomalies create a depression in the north and uprising in the south.

2D residual anomaly map (Fig. 1c) of the study area revealed residual magnetic intensity, which ranges from -121.1 to 134.9 nT. This indicates the study area is characterized with low and high magnetic signature. Residual magnetic fields are used extensively to bring into focus local features, which tend to be obscured by the broad features. Areas of strong positive anomalies likely indicate a higher concentration of magnetically susceptible minerals, while areas with broad magnetic lows are likely of lower susceptibility minerals. This is in line with the work of Ayigun *et al.*, 2022. On the other hand, Monguno residual gravity anomaly map (Fig. 1d) identifies high gravity anomalies in the northeast

and southern parts of the area respectively. High gravity anomaly noticed in northeast, however is not seen in Bouguer anomaly map (Fig.1b). This could be as result of the removal of the regional gravity response from the Bouguer anomaly map. Low gravity anomalies observed in northwest and at extreme edges in the south, indicate that the areas are composed of sediments or materials, which are less dense. The high gravity anomaly could be attributed to intrusive dense bodies.

Aeromagnetic source parameter imaging estimated the depth of the area to ranges from 549.4 to 4317.3 m, with an average depth value of about 1762.7 m. This shows the area is made of both shallow and deep depths. The shallow depths vary from 549.4 to 1164.8 m with an average depth value of about 893.4 m, while the deep depth ranges from 2544.1 to 4317.3 m with an average depth value of about 3259.4 m. The north and southern parts of the area are dominated by shallow depths, while the deep depths are identified in the central region and southeast respectively. This is in line with the work of Wobodo *et al.*, 2021

The aerogravity source parameter imaging depth map (Fig. 2b) shows that the depth to basement ranged from 821.4 to 5031.2 m, with an average value of 2917.7 m. The shallow depths range from 821.4 to 2043.2 m with an average value of about 1512.2 m; while the deep depths vary from 4300.5 to 5031.2 m with an average value of about 4674.3 m. Shallow depths are seen in the northeast, southwest and central region. This shallow depth could be attributed to shallow gravity bodies. Areas with deep depths, which are associated with deep lying gravity bodies, are observed in the north and south. The results obtained by the two methods are closely related.

The results of the aeromagnetic forward and inverse modeling as given in Figure 3(a - b) and

summarized on Table 1 show that the estimated depths from the forward and inverse modeling are 2296 and 1321 m, with susceptibility values of 0.0170 and 0.01 for P1 and P2 respectively. These indicate presence of mineral like Sandstone and Shale respectively. Similarly, the estimated depth from the forward and inverse modeling of aerogravity as shown in Figure 3 (c) is 1729 m for P1, with density value of 2.510 g/cm³, which indicates the presences of Kaolinite/ Gypsum. Thompson and Oldfield, 1986 and Telford *et al.*, 1990

CONCLUSION

The aeromagnetic and aerogravity data of the study area have been interpreted qualitatively and quantitatively. The qualitative interpretation shows that the area is characterized by both low and high frequency magnetic and gravity signatures. The aeromagnetic source parameter imaging estimated the sedimentary thickness of 3259.4 m, while the aerogravity source parameter imaging estimates the sedimentary thickness of 4674.3 m. On the other hand, the forward and inverse modeling technique estimated the depth to basement as: 2296, 1321, 1729 m respectively and identify the following minerals sandstone, shale, kaolinite and gypsum in the area.

Acknowledgment

Nigerian Geological Agency Abuja is acknowledge for releasing the data

REFERENCES

- Adekoya, J. A; Ola, P. S and Olabole, S.O. (2014). Possible Bornu basin hydrocarbon habitat: A reviews. *International Journal of Geosciences*, 5, 983-996.
- Adewumi, T., Salako, K. A., Salami, M. K., Mohammed, M. A. and Udensi, E. E. (2019). Estimation of sedimentary thickness using spectral analysis of aeromagnetic data o v e r parts of Bornu basin, Northeast, Nigeria. *Asian Journal of Physical and Chemical Sciences*, 2(1), 1- 8.
- Ajana, O., Udensi, E.E, Momoh, M., Rai, J.K. and Muhammad, S.B. (2014). Spectral Depths Estimation of Subsurface Structures in Parts of Borno Basin, North eastern Nigeria, using Aeromagnetic Data. *Journal of Applied Geology and Geophysics* 2(2):55-60.
- Akiishi, M, Udochukwu, B.C and Tyovenda, A, (2019). Determination of hydrocarbon potentials in Masu area northeastern Nigeria using forward and inverse modeling of aeromagnetic and aerogravity data. *SN Applied Sciences*,1(8), 911.
- Akiishi, M., and Ankeli, G. O.(2020). Investigation of solid mineral deposit in gubio, Nigerian sector of Chad basin using aeromagnetic and aerogravity forward and inverse modeling. *International Astronomy and Astrophysics Research Journal*, 2(2), 28-40, 2020; Article no.IAARJ.57440
- Ayigun, S, Hamid, K. Y and Omoniyi, O.T (2022). Review: Spectral analysis of aeromagnetic data. *International Research Journal of Pure and Applied Physics*, (9) 1, 1- 11
- Hsu, N.C.; Herman, J. R.; Bhartia, P.K.; Seftor, C.J.; Torres, O.; Thompson, A.M.; Gleason, J.F.; Eck, T.F., and Holben, B.N. (1996). Detection of biomass burning smoke from TOMS measurement. *Geophysics Research letters*, 23,745- 748
- Ijeh, B. I, Ohaegbuchi, H. E and Okpetue, P. C. (2019). Integration of aeromagnetic data and land sat imagery for structural analysis: A case study of Awgu in Enugu State, South-Eastern, Nigeria world news of natural sciences. *An International Scientific Journal WNOFNS*, 18(2), 79-105.
- Kehinde, S, Ishola, B. C, Okoye, L .A, and Kayode F. O (2019). Analysis of aeromagnetic anomalies of the North-eastern Nigerian part of the Chad basin. *Journal of Research and*

- Review in Science*, 4, 36–43.
- Nwobodo, A. N., Ikeri, H. I. and Chikeleze, P. C. (2021). Interpretation of aeromagnetic data of Guzabure and its environs Chad basin Northeastern Nigeria, using source parameter imaging *The International Journal of Engineering and Science (IJES)*, 10 (5), 45-50
- Nabighian, M. N. (1972). The analytic signal of two dimensional magnetic bodies with polygonal cross-section: Its properties and use for automated anomaly interpretation. *Geophysics*, 37(3), 507- 517.
- Obaje, P. T. (2009). *Geology and Mineral Resources of Nigeria*, Berlin: Springer Publisher
- Obiora, D. N., Ossai, M. N., and Okwohi, E. (2015). A case study of aeromagnetic data interpretations of Nsukka area, Enugu State, Nigeria for hydrocarbon exploration. *International Journal of Physical Science*, 10(17), 503– 519.
- Odebode, M.O. (2010). Handout on geology of Borno (Chad) Basin Northeastern Nigeria.
- Okosun, E. A. (1995). Review of Borno Basin. *Journal of Mining and Geology*, 31(2), 113-172.
- Rabo, Y., Bonde, D. S., Bello, A. and Abubakar, I. (2021). Estimation of basement depth of eastern part of Sokoto sedimentary basin northwestern Nigeria. *Science Journal of Advanced and Cognitive Research*, 2(1), 22-29
- Salako, K. A. and Udensis, E. E. (2013). Spectral depth analysis of parts of upper Benue trough and Borno basin, North – East Nigeria, using aeromagnetic data. *International Journal of Science and Research*, 2(8), 48-55.
- Sani, B Udensi, E.E, Salako, K. A. and Adetona, A. A. (2019). Determination of depth to magnetic basement using spectral analysis of aeromagnetic data over Biu Plateau basalt and Yola Sub - basin, North East Nigeria, *International Journal of Science and Research (IJSR)*, 7.426
- Telford, W.M., Geldart, L.P. and Sheriff, R.E. (1990). *Applied geophysics*, 3rd Edition. UK, Cambridge: University Press Cambridge.
- Thompson, R. and Oldfield, F. (1986). *Environmental magnetism*. London: Allen and Unwin
- Thurston, J. B. and Smith, R.S. (1997). Automatic conversion of magnetic data to depth dip and susceptibility contrast using the SPI™ methods. *International Journal of Geophysics*, 62 (3), 807– 813.
- Udochukwu, B. C, Akiishi, M and Tyovenda, A. A. (2019). Estimation of geothermal gradient and heat flow for determination of geothermal energy sources in Monguno Area Northeastern Nigeria. *Journal of Geography, Environment and Earth Science International*, (1), 1-8.